Available online at www.sciencedirect.com
SCIENCE DIRECT®
Analytical Biochemistry 355 (2006) 50–61
ANALYTICAL BIOCHEMISTRY
www.elsevier.com/locate/yabio

DNA methylation mapping by tag-modified bisulfite genomic sequencing

Weiguo Han [a], Stephane Cauchi [a], James G. Herman [b], Simon D. Spivack [a,c,d,*]

[a] *Laboratory of Human Toxicology & Molecular Epidemiology, Wadsworth Center, NYS Department of Health, Albany, NY 12201, USA*
[b] *Oncology Center, Johns Hopkins Medical Institutions, Albany, NY 12201, USA*
[c] *Pulmonary & Critical Care Medicine, Albany Medical College, Albany, NY 12201, USA*
[d] *SUNY School of Public Health, Albany, NY 12203, USA*

Received 26 January 2006
Available online 2 June 2006

Abstract

A tag-modified bisulfite genomic sequencing (tBGS) method employing direct cycle sequencing of polymerase chain reaction (PCR) products at kilobase scale, without conventional DNA fragment cloning, was developed for simplified evaluation of DNA methylation sites. The method entails subjecting bisulfite-modified genomic DNA to a second-round PCR amplification employing GC-tagged primers. Qualitative results from tBGS closely correlated with those from conventional BGS ($R = 0.935$, $p = 0.002$). In application, the intertissue and interindividual CpG methylation differences in promoter sequence for two genes, *CYP1B1* and *GSTP1*, were then explored across four human tissue types (peripheral blood cells, exfoliated buccal cells, paired nontumor–tumor lung tissues), and two lung cell types in culture (normal NHBE and malignant A549). Predominantly conserved methylation maps for the two gene promoters were apparent across donors and tissues. At any given CpG site, variation in the degree of methylation could be determined by the relative height of C and T peaks in the sequencing trace. Methylation maps for the *GSTP1* promoter diverged between NHBE (unmethylated) and A549 (completely methylated) cells in a previously unexplored upstream region, correlating with a 2.7-fold difference in GSTP1 mRNA expression ($p < 0.01$). The tBGS method simplifies detailed methylation scanning of kilobase-scale genomic DNA, facilitating more ambitious genomic methylation mapping studies.

Keywords: DNA methylation; Bisulfite genomic sequencing; CYP1B1; GSTP1; Exfoliated cells

Methylation of cytosines located 5′ adjacent to guanosine is known to have a repressive effect on the expression of many eukaryotic genes [1–6]. Aberrant methylation of normally unmethylated CpG islands has been documented as a relatively frequent event in experimentally immortalized and transformed cells and has been clearly associated with transcriptional inactivation of defined tumor suppresser genes in human cancers [7,8]. Hundreds of CpG islands are now known to exhibit the characteristic of hypermethylation in tumor cells [9]. Therefore, mapping of methylation patterns in CpG islands has become important for elucidating both normal and pathologic gene expression events.

The cytochromes P450 are important phase I bioactivating carcinogen metabolism enzymes and have been hypothesized to be responsible, in part, for interindividual differences in susceptibility to chemically induced disease [10–15]; CYP1B1 is among the most highly expressed P450 enzymes in human lung and human breast, and it bioactivates both polyaromatic hydrocarbons and estradiol to highly mutagenic species. Glutathione *S*-transferases (GSTs)[1] are phase II deactivating enzymes critically involved in DNA protec-

* Corresponding author. Fax: +1 518 486 1505.
E-mail address: spivack@wadsworth.org (S.D. Spivack).

[1] *Abbreviations used*: GST, glutathione *S*-transferases; BGS, bisulfite genomic DNA sequencing; MSP, methylation-specific PCR; PBMC, peripheral blood mononuclear cell; EBC, exhaled breath condensate; NHBE, normal human bronchial epithelial; RT, reverse transcription.

0003-2697/$ - see front matter © 2006 Elsevier Inc. All rights reserved.
doi:10.1016/j.ab.2006.05.010

tion from electrophilic metabolites of carcinogens, reactive oxygen, nitrogen, lipid species, and chemotherapeutic agents. *GSTP1* is the most highly expressed *GST* in the human lung and upper airway [16,17]. Observational studies on normal tissue expression patterns for both *CYP1B1* and *GSTP1* gene products suggest interindividual variation over several orders of magnitude, unexplained by measured environmental exposures [16–18]. Variation in regulatory region features, including promoter genetic polymorphisms, transcription factor levels, and epigenetic features, are hypothesized to vary across individuals. To our knowledge, no detailed survey of variation in normal tissue epigenetic features has been performed across kilobase-level expanses of promoter DNA sequence to explain this interindividual and intertissue variation; this laboratory set out to do so.

Several methods to determine the methylation status of cytosines in DNA have been developed [19]. These include digestion with methylation-sensitive restriction enzymes, as in restriction landmark genomic scanning [20], oligonucleotide arrays [21], pyrosequencing [22], or MS-based primer-extension-based methods [23], in addition to bisulfite genomic DNA sequencing (BGS) and methylation-specific PCR (MSP). MSP is now an established technology for the monitoring of abnormal gene methylation in selected gene sequences [24]. MSP is a discontinuous method for assaying DNA sequence; it generally samples oligomer annealing sites of approximately 20 bases in and around known methylation CpG sites. The technique relies on bisulfite chemical treatment of genomic DNA, to chemically convert unmethylated cytosines to uracils, and the replacement of uracil, in the subsequent PCR, with thymidines. The careful design of MSP primers allows, in separate uniplex reactions, either a match or a mismatch at the CpG site in question and therefore either a successful or an unsuccessful PCR with a categorical readout, either positive or negative. Both qualitative and quantitative MSP [25–29] require prior genomic methylation screening to direct primer design to appropriate specific target sequence for analysis. Matrix-assisted laser desorption ionization-time of flight mass spectrometry has recently been reported as an alternative genomewide methylation mapping approach [30] but may be resource intensive from procedural, instrumentation, and informatics perspectives.

BGS offers a continuous readout of the entire, detailed, base-by-base methylation map of a genomic DNA sequence [31,32]. The technique also relies on initial bisulfite modification of DNA and, as a final step, direct cycle sequencing of the resulting PCR-amplified sequence. PCR primers are designed external to potential methylation sites. However, because of the bisulfite conversion of unmethylated C $\Rightarrow$ U in the template, there is a paucity of C (sense) or G (antisense strand) nucleotides in the PCR product. Thus, there is a skewed (low) GC content, rendering direct cycle sequencing extremely challenging and often uninterpretable.

Conventional bisulfite sequencing commonly requires the cloning of PCR product for two reasons: First, the incorporation into the plasmid vector allows skewed GC content to be compensated for by the external plasmid sequence. Second, this approach provides precise methylation patterns of individual DNA molecules, overcoming tissue heterogeneity issues affecting methylation patterns at individual CpG sites. However, this requirement makes conventional BGS quite time consuming and labor intensive, and it precludes large-scale surveillance studies across multiple regions, genes, tissues, and donors.

We report a tag-modified BGS method (tBGS), which yields a 5′ and 3′ GC-tagged PCR product that sufficiently enhanced the GC content to allow successful direct-cycle sequencing. Essentially, we hypothesize that the GC-rich tag incorporates dCTP and dGTP into the PCR products and therefore produced a more evenly distributed nucleotide stoichiometry in the sequencing reaction. Cloning procedure was avoided. Tracings contained no detectable background. We applied the tBGS method to show its utility in the mapping of methylation patterns, in the promoters of two carcinogen-metabolizing genes, across human tissue types and cells, including exfoliated and exhaled specimens, and across individual subjects.

Materials and methods

Subjects

A total of 46 Caucasian subjects were analyzed in the present study, under ongoing protocols approved by both the Albany Medical Center and the New York State Department of Health Institutional Review Boards. Informed consent was explicit, and privacy was protected by stripping of traceable identifiers from clinical samples. The group consisted of 18 current smokers, 22 former smokers, and 6 never smokers; smoking status was confirmed by plasma nicotine and cotinine biomarkers and by self-reported history [16,17]. Both peripheral blood mononuclear cell (PBMC) and mouthwash-exfoliated buccal cell samples were obtained from 40 individuals, of whom 27 had a new diagnosis of lung cancer (untreated) and 13 were noncancer controls. For the 10 subjects donating lung tissue, pathologically confirmed non-small-cell lung tumor ($n = 9$) or benign bronchial adenoma ($n = 1$) tissue was paired with adjacent histologically nontumor tissue; 5 of these 10 individuals were among the 40 providing both blood cells and buccal cells. One additional donor (never smoker) provided exhaled breath condensate (EBC). Subjects were interviewed and peripheral blood and mouthwash-exfoliated cells were collected preoperatively before any clinically indicated diagnostic or therapeutic lung resectional surgery was performed.

Peripheral blood mononuclear cell and buccal cell collection

Phlebotomy was performed by standard clinical technique; isolation of PBMC was performed in standard fashion using a Ficoll gradient technique as described [33].

Mouth-washed buccal cell specimens were obtained by having the subject rinse the mouth thoroughly with 7.5 ml of a commercially available standard mouthwash (Scope; Proctor & Gamble) for 10–15 s, with deposition of the resulting rinse into a sterile container for storage at −80 °C until subsequent analysis. Blood and buccal specimens were collected during the same session and within 24–48 h of the relevant surgical lung biopsy and/or resection.

Exhaled breath condensate collection

One subject volunteered to donate EBC, which was collected in an EcoScreen exhaled breath condenser (Jaeger, Hoechberg, Germany) during quiet tidal volume breathing. Approximately 1.0 ml of EBC was collected in the condenser portion (<0 °C) of the device during 10 min of normal tidal breathing; this volume contained 250–500 ng genomic DNA on replicate samples. The system offers virtually no resistance to tidal volume breathing. This collection procedure was repeated at two time points.

Cell culture

Normal human bronchial epithelial (NHBE) cells were primary, nontransformed, and nonimmortal and were obtained from a commercial source (BioWhittaker, Inc., Walkersville, MD). NHBE cells were maintained and cultured in BEGM medium (BioWhittaker, Inc.) as previously described [29]. A549 cells (lung adenocarcinoma cells) from ATCC were cultured in F12K nutrient mixture (Invitrogen) supplemented with 10% fetal bovine serum and 10 μg/ml gentamicin at 37 °C in a humidified 5% CO_2 atmosphere.

Preparation of genomic DNA

Genomic DNA was isolated using a standard isolation kit (Gentra Systems, Minneapolis, MN) according to the manufacturer's recommendations. Briefly, cell lysis, where applicable, was followed by RNase and proteinase K treatment, isopropanol precipitation, ethanol washing, and storage in a hydration solution at −20 °C.

Bisulfite modification

Genomic DNA was modified by EZ DNA Methylation Kit (Zymo Research, Orange, CA). Briefly, 1 μg of DNA in a volume of 50 μl was denatured by 5 μl M-dilution buffer for 15 min at 37 °C. Bisulfite-containing CT-Conversion Reagent (100 μl) was added and mixed, and samples were incubated at 50 °C for 18 h. Modified DNA was purified by Zymo-Spin 1 Column and used immediately or stored at −20 °C.

GC tag-modified bisulfite genomic DNA sequencing

The sense strand of bisulfite-modified genomic DNA was amplified with primers specific for the *CYP1B1* and *GSTP1* promoters (Table 1). For the *CYP1B1* promoter, PCR conditions were 95 °C for 15 min, 5 cycles of 95 °C for 10 s, 54 °C for 30 s, 72 °C for 1 min, 35 cycles of 95 °C for 10 s, 48 °C for 30 s, 72 °C for 1 min, and finally 5 min at 72 °C. For the *GSTP1* promoter, conditions were 95 °C for 15 min, 40 cycles of 95 °C for 30 s, 50 °C for 30 s, 72 °C for 1 min, and finally 7 min at 72 °C. The PCR mixture contains 1 × buffer (Qiagen, Valencia, CA) with 1.5 mM $MgCl_2$, 1 μM each promoter-specific sense and antisense primer,

Table 1
First-round methylation PCR primers for *CYP1B1* and *GSTP1* promoters

	Primer	Sequence	Product	Region
CYP1B1	1B1MF1B	TTT GGAGTG GGATTTGGTGG	P1	1481–1921[a] (−1589 ~ −1149)[b]
	1B1MR4	ACTCTATAATCTTCCTAAAC		
	1B1MF2	GTTTAGGAAGATTATAGAGT	P2	1902–2529 (−1168 ~ −541)
	1B1MR2ab	AATCCCTAAAAATAACC(A/G)CTCC		
	1B1MF3	TTTGTGTGTTTAAGTATTGT(T/C)G	P3	2471–2819 (−599 ~ −251)
	1B1MR5	AACCACCTCCAATCAAAAC		
	1B1MF4	G(C/T)GGAGAGGGAAGGGAGGT	P4	2696–3090 (−374 ~ +20)
	1B1MR3ab	CACAACTAAAATC(A/G)CAAAA		
GSTP1	GSTP1MF1	ATATTTAGGGAAAATAGGAAAGGATTTA	P5	30–333 (−1856 ~ −1553)
	GSTP1MR1	CACAAACAAAAAAACAACAAACACTATA		
	GSTP1MF2	TTTAAGGTATAGTTATTAAAAGGAA	P6	729–1136 (−1158 ~ −751)
	GSTP1MR2	TCCCAAAATACTAAAATTACAAAC		
	GSTP1MF3	TTTAGAATTTTAAATAAAAGTTGGA	P7	1067–1353 (−820 ~ −534)
	GSTP1MR3	ATAACCCAAACTAAAATACAATAAC		
	GSTP1MF4	GGTTGAAGTAGAATTGTTTGAATT(C/T)G	P8	1269–1506 (−618 ~ −381)
	GSTP1MR4	TAAAAACCACTTAAAAAAAAAAAAATTAC		
	GSTP1MF5	GTAATTTTTTTTTTTTTAAG(C/T)TGGTTTTTA	P9	1478–1683 (−409 ~ −204)
	GSTP1MR5	CCTTTCCCTCTTTCCCAAAT		
	GSTP1MF6	TTGTTGTTTGTTTATTTTTTAGGTTT	P10	1630–1966 (−257 ~ +80)
	GSTP1MR6	ACTAAAAACTCTAAACCCCATCCC		

All primers are 5′ → 3′ oriented.
[a] Positions refer to GenBank sequence (U56438 for CYP1B1 and AY324387 for GSTP1).
[b] Position refers to transcription initiation site.

Table 2
Second-round PCR primers for *CYP1B1* and *GSTP1* promoters

Template	Primer	Sequence	Region
P1	CF1	**CCACTCACTCACCCACCC**TTTGGAGTGGGATTT	1481–1718
	MR1718	**GGGTGGGAGGTGGGAGGG**ATATCTAATTAACCAAA	(−1589 ~ −1352)
P1	MF1677	**CCACTCACTCACCCACCC**TTTGATGAAGTTAGTAT	1677–1921
	GR1	**GGGTGGGAGGTGGGAGGG**ACTCTATAATCTTCC	(−1393 ~ −1149)
P2	CF2	**CCACTCACTCACCCACCC**GTTTAGGAAGATTAT	1902–2327
	MR2327	**GGGTGGGAGGTGGGAGGG**AACCTAAAAAAACTAAC	(−1168 ~ −743)
P2	MF2151	**CCACTCACTCACCCACCC**AGGGATATGATTGGAGT	2151–2529
	GR2	**GGGTGGGAGGTGGGAGGG**AATCCCTAAAAATAA	(−919 ~ −541)
P3	CF3	**CCACTCACTCACCCACCC**TTTGTGTGTTTAAGT	2471–2819
	GR3	**GGGTGGGAGGTGGGAGGG**AACCACCTCCAATCA	(−599 ~ −251)
P4	CF4	**CCACTCACTCACCCACCC**GC/TGGAGAGGGAAGGG	2696–2885
	MR2885	**GGGTGGGAGGTGGGAGGG**ACCAACAAACTTTCATAA	(−374 ~ −185)
P4	MF2801	**CCACTCACTCACCCACCC**GTTTTGATTGGAGGTGGT	2801–3090
	GR4	**GGGTGGGAGGTGGGAGGG**CACAACTAAAATCA/GC	(−269 ~ −+20)
P5	GSTP1MFT1	**CCACTCACTCACCCACCC**TAGGAAAGGATTTA	44–319
	GSTP1MRT1	**GGGTGGGAGGTGGGAGGG**CAACAAACACTATA	(−1842 ~ −1539)
P6	GSTP1MFT2	**CCACTCACTCACCCACCC**GTTATTAAAAGGAA	739–1126
	GSTP1MRT2	**GGGTGGGAGGTGGGAGGG**CTAAAATTACAAAC	(−1147 ~ −741)
P7	GSTP1MFT3	**CCACTCACTCACCCACCC**AAATAAAAGTTGGA	1078–1342
	GSTP1MRT3	**GGGTGGGAGGTGGGAGGG**TAAAATACAATAAC	(−809 ~ −523)
P8	GSTP1MFT4	**CCACTCACTCACCCACCC**ATTGTTTGAATT(C/T)G	1281–1491
	GSTP1MRT4	**GGGTGGGAGGTGGGAGGG**AAAAAAAAAATTAC	(−606 ~ −366)
P9	GSTP1MFT5	**CCACTCACTCACCCACCC**TTAAG(C/T)GGTTTTTA	1493–1677
	GSTP1MRT5	**GGGTGGGAGGTGGGAGGG**CCTCTTTCCCAAAT	(−394 ~ −198)
P10	GSTP1MFT6	**CCACTCACTCACCCACCC**TATTTTTTAGGTTT	1642–1956
	GSTP1MRT6	**GGGTGGGAGGTGGGAGGG**CTAAACCCCATCCC	(−245 ~ +70)

All primers are 5′ → 3′ oriented; boldfaced letters indicate tag sequence.

5 U of HotStar Taq polymerase (Qiagen), and 50–100 ng bisulfite-modified genomic DNA. The PCR thermal profiles were programmed into a Perkin–Elmer 9700 thermocycler. These first-round PCR products were then used as template (1 μl) and reamplified by tagged primers (Fig. 2, Table 2).The second-round PCR conditions for *CYP1B1* were 95 °C for 15 min, 35 cycles of 95 °C for 10 s, 55 °C for 20 s, 72 °C for 20 s, and finally 7 min at 72 °C. The second-round PCR conditions for *GSTP1* were 95 °C for 15 min, 40 cycles of 94 °C for 30 s, 60 °C for 30 s, 72 °C for 1 min, and finally 7 min at 72 °C. PCR products were then purified with a Gel Extraction Kit (Qiagen) and subjected to direct cycle sequencing on a Perkin–Elmer Biosystems ABI Model 3100/3700 automated DNA sequencer, using the tag-targeted sequencing primers 5′-CCACTCACTCACCCACCC-3′ (forward), and 5′-GGGTGGGAGGTGGGAGGG-3′ (reverse). All samples were analyzed in duplicate, from bisulfite modification to sequencing. Manual review of sequence chromatograms containing two peaks at any one CpG locus was performed by measuring the peak height of the C (or antisense G) versus the combined height of the C + T peaks and generating a C/C + T (or antisense A/A + G) peak height representing the methylated fraction of DNA molecules, as a percentage [34,35].

Conventional bisulfite genomic sequencing

Methylation status was verified in one fragment of each of the two genes by cloning the first-round PCR product from each, derived from the same sample of bisulfite treated genomic DNA, into PCR-2.1-TOPO vector (Invitrogen) and performing direct cycle sequencing on 10 clones per fragment.

Primer design principles for successful tBGS

Design principles for the first-round PCR primer are as follows. (1) CpG sites in the primer annealing site should be avoided. (2) If they are unavoidable, however, degenerate primers employing C/T for in the forward primer and G/A for G in the reverse primer can be employed. (3) Amplification is of only one strand (e.g., the sense strand) of the bisulfite-treated genomic DNA (4) For any given strand, the forward primer should contain multiple Ts, deriving from non-CpG-site bisulfite-converted Cs near the 3′ end, so as to distinguish bisulfite-converted target strands from other (contaminating or incompletely converted) strands. The same principle (analogously using multiple As) holds for the reverse primer. (5) Higher annealing temperatures (>50 °C) are better for specific amplification.

Design principles for the second-round PCR, using GC-tag-modified primers, are as follows. (1) GC tag length of 18–22 bases, containing at least 50% C (for forward primer) or G (for reverse primer), has proven successful; the upper limit of tag length has not yet been determined. (2) The sequence-specific region of the tagged oligo primer is most easily limited to approximately 15–20 bases, yielding a tagged primer <40–45 bp in length, which is compatible

with standard oligomer synthesis purity constraints. (3) The PCR product length is usually limited to 200–300 bp, such that a 20-base tag at each end can enhance GC content of the PCR product to greater than 10–20%.

Verification by conventional BGS

Bisulfite-treated genomic DNA from single-donor NHBE cells and single-donor A549 cells was PCR-amplified for both *CYP1B1* and *GSTP1* promoters, using primer pairs 1B1MF1B, 1B1MR4 and GSTP1MF1, GSTP1MR1, respectively. Each fragment was then cloned into TOPO T/A vector (Invitrogen). Ten colonies of each product were selected for sequencing. To determine the sensitivity of tBGS and conventional BGS in CpG methylation monitoring, we mixed known completely methylated and completely unmethylated DNA templates in different ratios, in 10% increments, for direct sequencing.

RNA-specific universal reverse transcription and PCR

Total RNA from NHBE and A549 cells was prepared by RNeasy Mini Kit (Qiagen), according to manufacturer's protocol. RT was performed by universal RT primer as previously described [36], avoiding genomic DNA–encoded false positives in the RT-PCR that are yielded by pseudogene-encoded sequences (e.g., *GSTP1* and *36B4* processed pseudogene sequences in genomic DNA).

Quantitative RT-PCR was performed in the LightCycler (Roche, Indianapolis, IN) thermocycler using *GSTP1* and *36B4* RNA-specific primers (Table 3). RT-PCR target transcript results were normalized to expression levels of the internal reference housekeeping gene *36B4* as previously described [17].

Table 3
Primers for quantitative RT-PCR

	Primer	Sequence
RT	URT	5′-AAC GAG ACG ACG ACA GAC TTT TTT TTT TTT TTT TTT A/C/G A/C/G A/C/G/T-3′
CYP1B1	DSF	5′-GCC ACT ATC ACT GAC ATC T-3′
	DSR	5′-CTT GCC TCT TGC TTC TTA TT-3′
GSTP1	UF2	5′-TCT CCT TCG CTG ACT ACA AC-3′
	UR	5′-AAC GAG ACG ACG ACA GAC-3′
36B4	UF1	5′-GAC AAT GGC AGC ATC TAC AA-3′
	UR	5′-AAC GAG ACG ACG ACA GAC-3′

Results

Direct sequencing of bisulfite-converted DNA–PCR products

Direct sequencing was initially attempted on the bisulfite-modified genomic DNA-derived PCR product for the *CYP1B1* promoter. This consistently yielded G background noise for reverse sequencing (Fig. 1) or C background noise for forward sequencing (Fig. 3, bottom). The background noise, which invariably corresponded to C or G signal, extended beyond the 3′ end of the template, presumably from unused ddCTP or ddGTP in the sequencing reaction mixture or possibly due to an alteration of gain by the sequencing instrument. Similar results were also observed for other sequence, including the *GSTP1* promoter. This phenomenon made it difficult to unambiguously distinguish the partially methylated CpG site from the unmethylated site, thus rendering direct-to-cycle sequencing interpretation of bisulfite-modified DNA–PCR products unreliable. This background phenomenon was also found when unmethylated CpG islands were examined [37,38].

Since the background C occurred in samples where the majority or all of the Cs had been eliminated by bisulfite treatment, we hypothesized that reintroduction of true C (or G) would restore appropriate signals for the C lane and thereby reduce background for this channel. To do so, we constructed primers which would include C (and G) in primer design, assuring that each base was represented in all PCR products prior to sequencing. We call these "GC tag primers."

Effect of GC-tag modification on direct sequencing of the PCR product

First-round PCR products were subjected to second-round PCR using tag-modified primers containing high C-

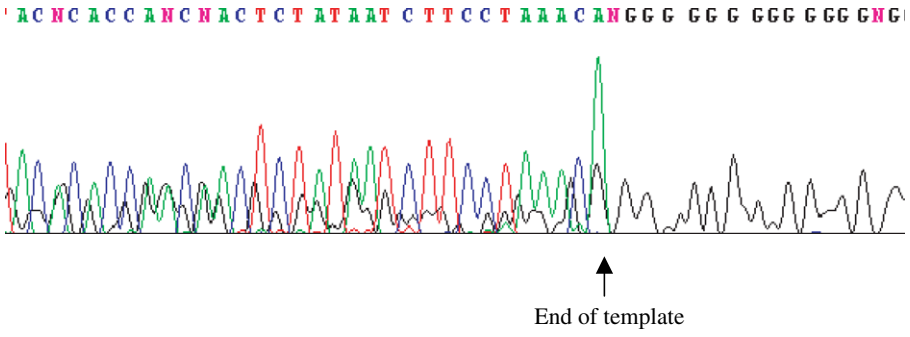

Fig. 1. Direct sequencing of the bisulfite-modified DNA–PCR product for *CYP1B1* gene promoter using standard-design PCR primers in the absence of cloning. Bisulfite genomic DNA was amplified by *CYP1B1*-promoter-specific standard-design primers (Table 1). PCR products were purified and subjected to direct cycle sequencing. The G background for reverse primer sequencing (black tracing) is apparent and extends beyond the 3′ end of the template sequence.

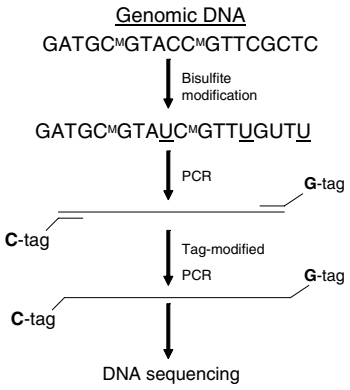

Fig. 2. Strategy of the GC-tag-modified bisulfite genomic sequencing approach. Initial bisulfite conversion of genomic DNA is amplified in a standard PCR in the first round, and then C- or G-tagged primers are employed to alter the base composition of the second-round PCR product. Standard sequencing is then reliably performed [USPTO patent pending No. 60/592337].

or G-content tags added to the 5′ or 3′ end (Table 2). Tag sequences were then used as sequencing primers as described under Materials and methods. Upon sequencing, a significant improvement in the clarity of chromatogram tracings was found (Fig. 3); partially methylated sequences (read as C/T) were clearly distinguishable from unmethylated sites (read as Ts in the sequencing reaction). We observed that ~5% or more of C and G integrated into both strands of the PCR product was sufficient to permit direct cycle sequencing of the PCR product without cloning. The sensitivity of the tBGS sequencing trace to methylated molecules was approximately 10% (Fig. 4).

Verification of tBGS by conventional BGS

For *GSTP1*, the tBGS methylation results were identical to conventional (cloning) BGS results (Fig. 4). No variation (homomethylation) in the *GSTP1* methylation strand haplotypes was observed by conventional BGS, and none was suggested by the tBGS sequence tracings.

Significant heterogeneity in methylation status in the *CYP1B1* haplotypes across DNA strands was detected by conventional BGS for both cell types. This implied that tBGS results reflected a pool of different methylation haplotypes, as expected (Fig. 5). Using conventional BGS as the reference method, tBGS sequence tracings of loci that showed some degree of methylation were called qualitatively positive. That positive signal was then graded according to tracing ratios (height of the unmethylated versus methylated tracing, in quintiles); Fig. 5 depicts this gradation of fraction methylated for tBGS as shades of gray. The degree of methylation ascertained by tBGS sequence chromatogram tracing height ratio was proportional to that fraction of cloned DNA molecules that were methylated ($R = 0.935$, $p = 0.002$), with the tBGS method generally estimating the fraction methylated to be 20–30% higher than that observed in the 10 conventionally sequenced clones (Fig. 5).

No false positive methylation calls were made by tBGS; areas free of methylation by tBGS were free of methylation when assayed by conventional BGS. The assessment of sensitivity of tBGS in CpG methylation monitoring, by mixing different ratios of methylated and unmethylated DNA templates in 10% increments, suggested that tBGS could routinely detect methylated CpG when present as ~10% of the total [Fig. 6]. The method routinely yielded clean baseline tracings, enabling this estimation of sensitivity.

Methylation mapping of the promoter of CYP1B1 and GSTP1

Screening was performed on an approximately 1.5-kb region of the promoter of the human *CYP1B1* gene and a

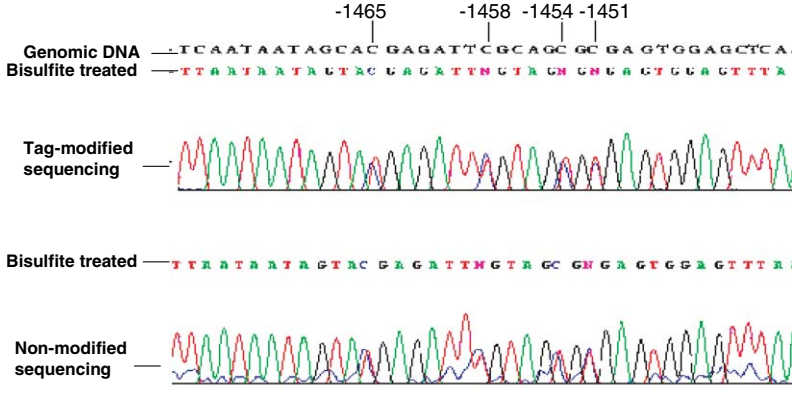

Fig. 3. Comparison of tag-modified (top tracing) and tag-unmodified (bottom tracing) PCR product sequencing. Bisulfite-converted genomic DNA was amplified by *CYP1B1*-promoter-specific primers (Table 1). After GC-tag modification by second-round PCR, the sense strand was sequenced. C background noise was consistently observed in the unmodified PCR product sequencing result, precluding methylation determinations at several positions in this short fragment. The positions refer to the transcription start site of the *CYP1B1* gene (U56438). Positions −1458 and −1454 can be seen to be hemimethylated: one allele is methylated, while the other is not, at each of the two sites.

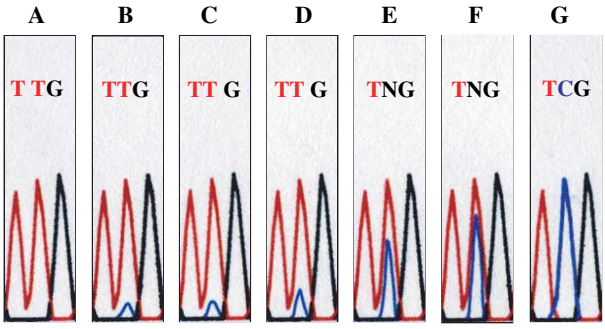

	mCpG (%)	uCpG (%)
A	0	100
B	10	90
C	20	80
D	30	70
E	40	60
F	50	50
G	100	0

Fig. 4. Tagged bisulfite genomic sequencing (tBGS) sensitivity to ^{m}CpG detection. Bisulfite treatment was performed on NHBE and A549 genomic DNA, where completely methylated or completely unmethylated genomic DNA for the most 5′ *GSTP1* promoter fragment as assessed by prior conventional (cloning) BGS studies was available. The respective fragments were then PCR-amplified and inserted in to a TA vector. The methylated and unmethylated clones that were verified by sequencing were then mixed together in 10% increments and subjected to direct sequencing. Representative CpG site sequences are displayed from A to G. (A) Known unmethylated CpG (uCpG) site from NHBE cells; (G) known methylated CpG (mCpG) site from A549 cell line. The method appeared capable of detecting 10% methylation, similar to the limits of detection for most direct cycle sequencing techniques, and qualitatively increased with increasing levels of methylation.

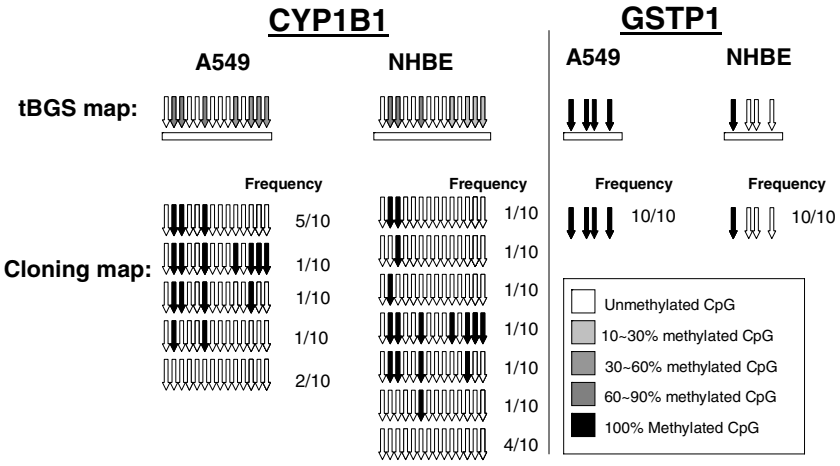

Fig. 5. Qualitative comparison of results from tBGS and conventional BGS. Genomic DNA was prepared from A549 and NHBE cells. Genomic DNA was bisulfite converted as described, and (left) the *CYP1B1* promoter was amplified by 1B1MF1B, 1B1MR4. PCR product was sequenced by tBGS strategy and the conventional (cloning) BGS method. Ten colonies were sequenced for the latter method. (right) *GSTP1* promoter was amplified by GSTP1MF1, GSTP1MR1 and analyzed in similar parallel fashion using the two methods. The results suggest consistency of methylation map (CpG site) patterns across the two methods, with the pool of DNA molecules analyzed by the tBGS method displaying results consistent with the single DNA molecules analyzed by conventional (cloning) BGS. Shades of gray (*CYP1B1* promoter) represent partial methylation, representative of the pool of differently methylated genomic DNA molecules at each CpG site, analyzed by the tBGS method. The *GSTP1* promoter showed no partial methylation by either technique.

1.8-kb region of the promoter of the *GSTP1* gene, inclusive of the vast majority of CpG sites in the respective 5′ flanking regions for these two genes. Among the various tissues surveyed from the donors, the methylation patterns in the promoters of *CYP1B1* and *GSTP1* were completely conserved, being consistent across all tissues and individuals (Table 4). However, in the *CYP1B1* promoter, all detected methylation represented partial methylation, ascertained according to second peaks in the sequencing trace at any site. The degree of methylation of CpG sites at −1465, −1458, −1454, and −1452, was about 20–30% in all tissues and NHBE cells, versus about 40–50% in A549 cells. CpG sites at −1537, −1535, and −1518 were about 80–90% methylated and those at −579 about 40–50% methylated in all tissues and cultured cells [Fig. 7].

Methylation pattern and expression of CYP1B1 and GSTP1 in NHBE and A549 cells

We examined the methylation patterns of the *CYP1B1* and *GSTP1* promoters in cultured NHBE and A549 cells. For both cell lines, the *GSTP1* promoter was methylated only in the region 5′ to a pentanucleotide repeat. In NHBE cells, the *GSTP1* promoter was unmethylated at a 10-CpG site area in the 5′ upstream region of the promoter (−1695 to −988); in contrast, this site was completely methylated in A549 cells (Fig. 7). Both findings were confirmed by direct standard BGS employing DNA cloning. No such methylation differences between the cell lines were found in the *CYP1B1* promoter; the *CYP1B1* promoter in A549 and NHBE showed the same methylation pattern as that observed in all tissue samples (Table 3).

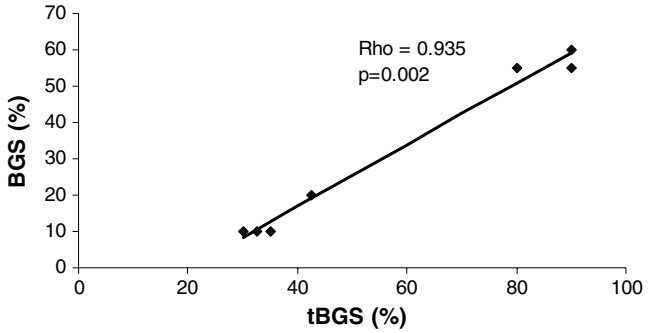

Fig. 6. Correlations of results from tBGS and conventional BGS. The −1589 to −1149 regions of *CYP1B1* promoter in NHBE and A549 were analyzed by both tBGS and conventional (cloning) BGS. The individual values of methylation degree were assessed by the relative heights of the C versus C + T tracings (or in the antisense direction, G/G + A) at each individual CpG site in the region (−1537, −1535, −1518, −1465, −1458, −1454, −1452) by tBGS. The fraction methylated in conventional BGS was performed by assessing the invariably monomorphic tracing yielded by single DNA molecule cloning and summing the result at each site with the other clones ($n = 10$ clones total). The paired results [e.g., tBGS (50% methylated) versus conventional BGS (3/10 or 30% methylated)] were correlated at each of the seven sites by the nonparametric Spearman correlation test, yielding Rho = 0.935, $p = 0.002$.

To assay the functional correlates of the methylation difference in the *GSTP1* promoter in NHBE and A549 cells, we determined the levels of mRNA transcript encoded by the respective genes, employing RNA-specific real-time quantitative RT-PCR. No difference in CYP1B1 mRNA expression was observed in the two cell lines (Fig. 8). However, GSTP1 mRNA expression was 2.7 times higher in the less-highly methylated NHBE cells than in the A549 cells (Fig. 8). This region has not previously been examined for methylation-associated changes in GSTP1 expression.

Discussion

To survey the CpG methylation patterns in human carcinogenesis, it is imperative to have available a simplified, higher-throughput analysis technique for surveying regions of interest [19,27,39–41]. Several methods have been devised for CpG methylation detection [19], but the most comprehensive approach to surveying large regions of DNA methylation at high resolution remains genomic sequencing [42,43]. Traditionally, this technique has required cloning of the PCR product into a vector for successful sequencing [31,41] in multiple clones (generally ⩾5–10), making it technically difficult, labor intensive, and unsuited to high-throughput investigations. In this study, we have described a simplified method, tBGS, which permits higher-throughput genomic DNA screening for the construction of methylation maps from noninvasively collected human specimens.

As illustrated by our results, this tBGS technique provides significant advantages over conventional BGS. Among these advantages, tBGS (1) enables the construction of methylation maps across kilobase-sized regions of DNA, at single-base resolution, while avoiding the need for DNA fragment cloning (this simplification reduces DNA isolation and sequencing 5- to 10-fold by circumventing the requirement for evaluation of 5–10 clones per DNA fragment for evaluation by conventional BGS), (2) employs second-round tag primers that are easily adapted from first-round genomic DNA primers, (3) uses two rounds of PCR, thus rendering it highly sensitive for trace genomic DNA application, as for typical small human specimen use, (4) tag sequences can be used as sequencing reaction primers, (5) has performance and internal control sequence advantages similar to those of conventional BGS, and (6) yields partial methylation results that correlate with those of conventional BGS. Performance in trace DNA sample situations was demonstrated in this study for a variety of tissues, including the demanding applications of exfoliated cells and exhaled breath samples.

The tBGS method has certain limitations. First, like conventional BGS and all other technologies employing conventional Sanger-based cycle sequencing chemistries, tBGS requires that a minimum of ~5–10% of chromosomal DNA be methylated at the site of interest to enable detection by the laser and capillary setup of the sequencing device (e.g., ABI 3100, 3700). This is not considered a major limitation, as the rarely methylated site (<5%) is unlikely to have major functional effects on the whole population of cells from which the DNA molecules are extracted. Where greater sensitivity is needed, biased PCR approaches, such as MSP, may be required. Second, localization of a specific methylated site to a particular DNA strand (or "allele") for construction of the methylation equivalent of haplotype is not possible without cloning, since the current tBGS tech-

Table 4
Methylated CpG site in the promoters of *CYP1B1* and *GSTP1*

Gene name	Number of CpG sites examined	Number of CpG sites methylated	Position of methylated CpG
CYP1B1	119	8	−579, −1452, −1454, −1458, −1465, −1518, −1535, −1537
GSTP1	82	30	−521, −531, −559, −561, −567, −570, −587, −623, −645, −684, −704, −715, −742, −747, −775, −787, −795, −863, −960, −988, −991, −1046, −1052, −1091, −1133, −1315, −1644, −1687, −1695, −1800

The data derive from both peripheral blood lymphocytes and exfoliated buccal cells from 40 individuals, from paired nonmalignant and malignant lung tissue specimens from 10 individuals, and from replicate exhaled breath condensate specimens from 1 individual. No intertissue or interindividual variation in promoter methylation was apparent for the two gene promoters studied. Positions refer to the respective transcription initiation site (GenBank: U56438 for *CYP1B1*, AY324387 for *GSTP1*).

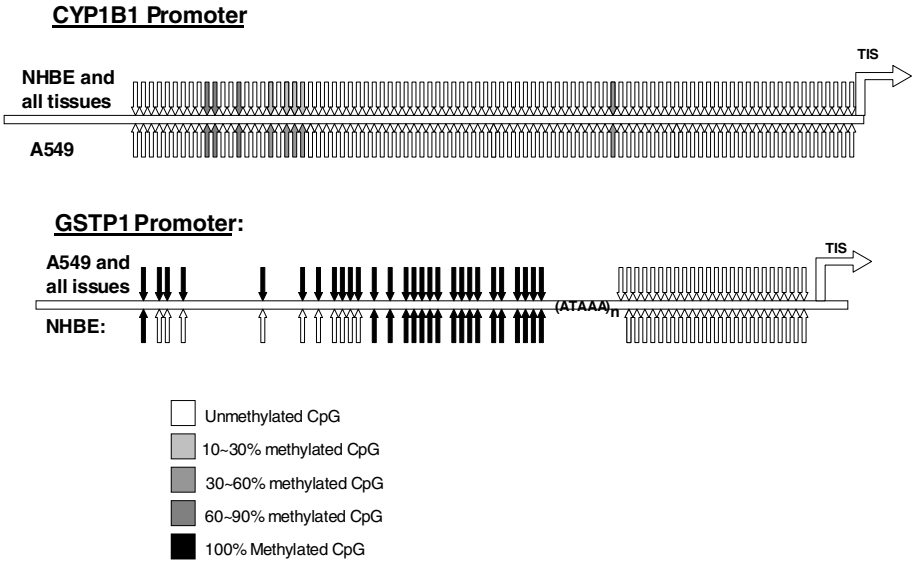

Fig. 7. *CYP1B1* and *GSTP1* promoter methylation maps of malignant A549 lung cells (and all other tissues examined), compared with normal human bronchial NHBE cells. For the *CYP1B1* promoter (top map), all tissues and donors had identical qualitative patterns. However, shades of gray depict partial methylation as being a common state. For the *GSTP1* promoter (bottom map), NHBE cells displayed a unique pattern of methylation for the 10 CpG sites found between positions −1695 and −988. The *GSTP1* promoter map was identical for the A549 cell line and for all buccal and PBMC data derived from 40 individuals, in addition to paired lung nontumor and tumor tissue derived from 10 individuals and exhaled breath condensate for the *GSTP1* promoter derived from 1 individual (Fig. 8).

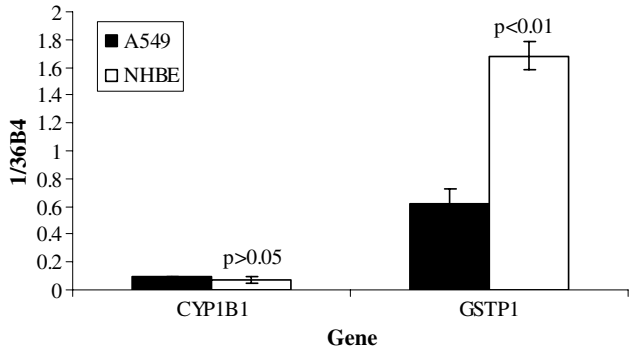

Fig. 8. mRNA expression of *CYP1B1* and *GSTP1* in NHBE and A549 cells. The RNA-specific RT-PCR revealed *GSTP1* transcript in NHBE cells to be 2.7-fold that in A549 cells. This difference was not observed for *CYP1B1* expression levels, where there were no methylation map differences in the two cell types. Target transcript levels (*CYP1B1* or *GSTP1*) are scaled to the internal reference housekeeper *36B4* (1/36B4). Data are shown as mean value ± SD ($n = 3$).

nique pools all template DNA molecules for sequencing (as is true in general of PCR product sequencing techniques and MSP). Third, the tBGS method is not quantitative, as currently implemented, for determination of the exact percentage of chromosomes methylated at any one CpG site; adaptations to render it semiquantitative can be envisioned, as piloted in this study, by measuring C/C + T peak height. Fourth, the method currently requires a two-step PCR amplification of the bisulfite-treated genomic DNA. While initial attempts have suggested the feasibility of reducing this to one round of PCR, using the original-design tagged primers (not shown), more development is required. It should be noted, however, that a disadvantage to the one-step approach relative to the two-step amplification is that less final PCR product is generated in the one-step approach. In that case, more of the original potentially precious human extract would be required to execute broad genomic methylation surveys.

This tBGS method is therefore useful in higher-throughput promoter methylation mapping from clinical samples to find potentially disease-related CpG methylation sites. We can envision the use of qualitative tBGS to survey larger regions of pooled DNA and follow up sites of interest with real-time quantitative MSP [28,29,39–41] or other methods, where precise quantitation and sensitivity are enhanced. Critical areas for experimental research on gene regulation might then be cloned.

To demonstrate the performance and translational utility of the tBGS assay, we focused on two commonly studied genes, *CYP1B1* and *GSTP1*. Wide interindividual variation in the mRNA expression of *CYP1B1* has been observed over 1000-fold despite identical exposures [17,18,44], and has been hypothesized to be responsible for interindividual differences in susceptibility to exogenous or endogenous mutagen-induced disease. On examination of the promoter methylation pattern in PBMCs and exfoliated buccal cells from 40 individuals (including the majority of the samples displaying the >1000-fold range in expression [17] and 10 paired lung tumor tissues and nontumor tissues, we found that only 8 of 119 CpGs were methylated in the *CYP1B1* promoter, in a highly conserved pattern for both CpG site location and degree of methylation at any given site, across individuals and tissues. There was no evidence of contamination to explain this result, as cloning of the first-round *CYP1B1* promoter PCR product revealed clearly differing

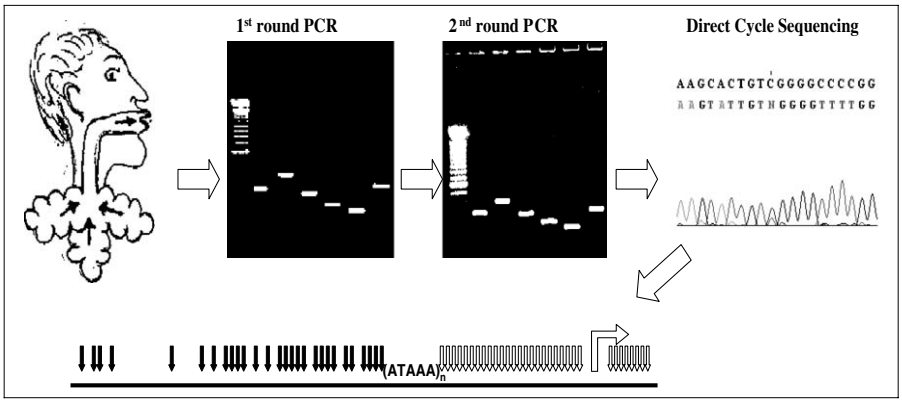

Fig. 9. *GSTP1* promoter PCR amplification from exhaled breath condensate (EBC) from one healthy donor was screened with the new tBGS technique. EBC was collected at three separate time points separated by months from the same subject with identical results. Genomic DNA isolation, bisulfite conversion, *GSTP1* promoter amplification in two steps (corresponding to the two gels), and direct cycle sequencing were performed using the tBGS approach. In the instance of *GSTP1*, six separate PCR amplifications (corresponding to each lane) were needed to cover the CpG sites from −1828 to +56, with the transcription start site as the reference. The first-round PCR allows amplification of bisulfite-treated DNA. The second-round PCR is performed with the tagged primers, permitting subsequent direct sequencing. Transcription start site is marked with a right-angle arrow.

patterns for A549 and NHBE cells. This result indicates that promoter methylation cannot easily explain the previously observed wide interindividual differences that we have observed in the expression of *CYP1B1* mRNA in these same tissue samples [17].

Promoter methylation has been demonstrated to be one of the factors implicated in the regulation of *GSTP1* gene expression in a wide range of human tissues [45]. When we examined the *GSTP1* promoter methylation pattern in PBMCs and buccal cells from 40 individuals and in 10 lung tumor and nontumor tissues, a consistent pattern was again seen; 30 of 82 CpG sites were completely methylated, the remainders were completely unmethylated, and this uniformly conserved pattern held across all tissue types assayed and across all individual subjects. We speculate that this conserved methylation pattern may be important in maintenance of *GSTP1* expression levels. This result again indicates that promoter methylation cannot easily explain the previously observed wide interindividual differences that we have determined in the expression of *GSTP1* in these same normal tissue samples [17]. In studies employing MSP techniques in tumors, *GSTP1* methylation was noted to be only rarely detected (in the limited region immediately surrounding the transcription start site) in non-small-cell lung tumors [25,46,47], and virtually never in normal tissues. Consistent with these MSP-based findings, the current tBGS-based studies did not detect methylation in the 3′ region of the *GSTP1* promoter.

In cell culture, however, the *GSTP1* methylation in normal lung (NHBE) cells differed both from that in malignant lung (A549) cells in culture, and from that in all the tissue specimens described above, including nontumor lung tissue. For the NHBE cells uniquely, the region (−1695 to −988) was unmethylated at a block of 10 CpG sites. As a corollary, *GSTP1* mRNA expression was 2.7-fold higher in NHBE cells than in A549 cells. Published MSP studies have not explored this region. Our result is consistent with findings of other studies, in that the degree of 5′ promoter methylation is inversely correlated with gene expression levels [28]; it suggests that a methylated region, quite remote from the transcription start site, may still modulate levels of gene expression. We elected not to experimentally pursue the use of global demethylating agents (e.g., 5-azacytidine), as the altered expression resulting from altering methylation at a whole-genome level does not confirm or refute the role of specific CpG site methylation in regulation at a specific promoter site. Rather, strategies for altering DNA methylation in a sequence-specific manner are currently being explored in the laboratory.

The ability to perform methylation mapping from trace amounts (100–250 ng) of genomic DNA in exhaled breath condensate in the one subject studied at multiple time points (Fig. 9) suggests the possibility of noninvasively sampling lung epithelium for "field cancerization," a novel approach under active study in the laboratory.

In summary, a simplified method for screening the detailed methylation status within large DNA regions and its application across human tissues and across donors has been demonstrated. It holds significant potential for facilitating the study of DNA methylation, in a variety of translational research contexts, including direct human studies in gene regulation and carcinogenesis, biomarker development, and therapeutic efficacy.

Acknowledgment

At the Wadsworth Center, the authors thank Shalini Kumar for organizational laboratory support, Dr. Laurence Kaminsky for administrative laboratory support, Matt Schudt and the Molecular Genetics Core for technical support in sequencing, the Biochemistry Core, and Dr. Adriana Verschoor for manuscript editing. At Albany Medical Center, research nurses Angela Sheehan, Kathy Mokhiber, and Ann Venezia contributed exemplary subject

recruitment, biospecimen collection, and organizational skills. Dr. Riivo Ilves, Thoracic Surgery and Dr. Tim Jennings, Anatomic Pathology, facilitated the procurement of surgical lung tissue, and clinical colleagues in Pulmonary & Critical Care Medicine kindly permitted the enrollment of their patients. This study was supported by NIH-R21 CA 94714 (to SDS), and NIH-R21 CA 10481 (to SDS), and NIH-R01 CA 106186 (to SDS).

References

[1] D. Takai, P.A. Jones, Comprehensive analysis of CpG islands in human chromosomes 21 and 22, Proc. Natl. Acad. Sci. USA 99 (2002) 3740–3745.
[2] A. Bird, The essentials of DNA methylation, Cell 70 (1992) 5–8.
[3] E. Li, C. Beard, R. Jaenisch, Role for DNA methylation in genomic imprinting, Nature 366 (1993) 362–365.
[4] K.D. Tremblay, J.R. Saam, R.S. Ingram, S.M. Tilghman, M.S. Bartolomei, A paternal-specific methylation imprint marks the alleles of the mouse H19 gene, Nat. Genet. 9 (1995) 407–413.
[5] A.D. Riggs, G.P. Pfeifer, X-chromosome inactivation and cell memory, Trends Genet. 8 (1992) 169–174.
[6] P.A. Jones, P.W. Laird, Cancer epigenetics comes of age, Nat. Genet. 21 (1999) 163–167.
[7] P. Adorjan, J. Distler, E. Lipscher, F. Model, J. Muller, C. Pelet, A. Braun, A.R. Florl, D. Gutig, G. Grabs, A. Howe, M. Kursar, R. Lesche, E. Leu, A. Lewin, S. Maier, V. Muller, T. Otto, C. Scholz, W.A. Schulz, H.H. Seifert, I. Schwope, H. Ziebarth, K. Berlin, C. Piepenbrock, A. Olek, Tumour class prediction and discovery by microarray-based DNA methylation analysis, Nucleic Acids Res. 30 (2002) e21.
[8] J.F. Costello, M.C. Fruhwald, D.J. Smiraglia, L.J. Rush, G.P. Robertson, X. Gao, F.A. Wright, J.D. Feramisco, P. Peltomaki, J.C. Lang, D.E. Schuller, L. Yu, C.D. Bloomfield, M.A. Caligiuri, A. Yates, R. Nishikawa, H. Su Huang, N.J. Petrelli, X. Zhang, M.S. O'Dorisio, W.A. Held, W.K. Cavenee, C. Plass, Aberrant CpG-island methylation has non-random and tumour-type-specific patterns, Nat. Genet. 24 (2000) 132–138.
[9] M. Esteller, P.G. Corn, S.B. Baylin, J.G. Herman, A gene hypermethylation profile of human cancer, Cancer Res. 61 (2001) 3225–3229.
[10] E. Aklillu, M. Oscarson, M. Hidestrand, B. Leidvik, C. Otter, M. Ingelman-Sundberg, Functional analysis of six different polymorphic CYP1B1 enzyme variants found in an Ethiopian population, Mol. Pharmacol. 61 (2002) 586–594.
[11] J. Lai, D. Vesprini, W. Chu, H. Jernstrom, S.A. Narod, CYP gene polymorphisms and early menarche, Mol. Genet. Metab. 74 (2001) 449–457.
[12] A.S. Wenzlaff, M.L. Cote, C.H. Bock, S.J. Land, A.G. Schwartz, GSTM1, GSTT1 and GSTP1 polymorphisms, environmental tobacco smoke exposure and risk of lung cancer among never smokers: a population-based study, Carcinogenesis 26 (2005) 395–401.
[13] S. Hohaus, A. Di Ruscio, A. Di Febo, G. Massini, F. D'Alo', F. Guidi, G. Mansueto, M.T. Voso, G. Leone, Glutathione S-transferase P1 genotype and prognosis in Hodgkin's lymphoma, Clin. Cancer Res. 11 (2005) 2175–2179.
[14] J.D. Hayes, D.J. Pulford, The glutathione S-Transferase supergene family: Regulation of GST and the contribution of the isoenzymes to cancer chemoprotection and drug resistance, Crit. Rev. Biochem. Mol. Biol. 30 (1995) 445–600.
[15] X. Hu, H. Xia, S.K. Srivastava, C. Herzog, Y.C. Awasthi, X. Ji, P. Zimniak, S.V. Singh, Activity of four allelic forms of glutathione *S*-transferase hGSTP1-1 for diol epoxides of polycyclic aromatic hydrocarbons, Biochem. Biophys. Res. Commun. 238 (1997) 397–402.
[16] S.D. Spivack, G.J. Hurteau, M.J. Fasco, L.S. Kaminsky, Phase I and II carcinogen metabolism gene expression in human lung tissue and tumors, Clin. Cancer Res. 9 (2003) 6002–6011.
[17] S.D. Spivack, G.J. Hurteau, R. Jain, S.V. Kumar, K.M. Aldous, J.F. Gierthy, L.S. Kaminsky, Gene-environment interaction signatures by quantitative mRNA profiling in exfoliated buccal mucosal cells, Cancer Res. 64 (2004) 6805–6813.
[18] J.C. Willey, E.L. Coy, M.W. Frampton, A. Torres, M.J. Apostolakos, G. Hoehn, W.H. Schuermann, W.G. Thilly, D.E. Olson, J.R. Hammersley, C.L. Crespi, M.J. Utell, Quantitative RT-PCR measurement of cytochromes p450 1A1, 1B1, and 2B7, microsomal epoxide hydrolase, and NADPH oxidoreductase expression in lung cells of smokers and nonsmokers, Am. J. Respir. Cell Mol. Biol. 17 (1997) 114–124.
[19] O. El Maarri, Methods: DNA methylation, Adv. Exp. Med. Biol. 544 (2003) 197–204.
[20] M.F. Fraga, M. Esteller, DNA methylation: a profile of methods and applications, Biotechniques 33 (2002) 636–649.
[21] D. Zhou, W. Qiao, L. Yang, Z. Lu, Bisulfite-modified target DNA array for aberrant methylation analysis, Anal. Biochem. 351 (2006) 26–35.
[22] J.-M. Dupont, J. Tost, H. Jammes, I.G. Git, De novo quantitative bisulfite sequencing using pyrosequencing technology, Anal. Biochem. 333 (2004) 127–199.
[23] J. Tost, P. Schatz, M. Schuster, K. Berlin, I.G. Gut, Analysis and accurate quantification of CpG methylation by MALDI mass spectrometry, Nucleic Acids Res. 31 (9) (2003) e50.
[24] J.G. Herman, J.R. Graff, S. Myohanen, B.D. Nelkin, S.B. Baylin, Methylation-specific PCR: a novel PCR assay for methylation status of CpG islands, Proc. Natl. Acad. Sci. USA 93 (1996) 9821–9826.
[25] S.V. Harden, Y. Tokumaru, W.H. Westra, S. Goodman, S.A. Ahrendt, S.C. Yang, D. Sidransky, Gene promoter hypermethylation in tumors and lymph nodes of stage I lung cancer patients, Clin. Cancer Res. 9 (2003) 1370–1375.
[26] S.E. Cottrell, J. Distler, N.S. Goodman, S.H. Mooney, A. Kluth, A. Olek, I. Schwope, R. Tetzner, H. Ziebarth, K. Berlin, A real-time PCR assay for DNA-methylation using methylation-specific blockers, Nucleic Acids Res. 32 (2004) e10.
[27] O. Topaloglu, M.O. Hoque, Y. Tokumaru, J. Lee, E. Ratovitski, D. Sidransky, C.S. Moon, Detection of promoter hypermethylation of multiple genes in the tumor and bronchoalveolar lavage of patients with lung cancer, Clin. Cancer Res. 10 (2004) 2284–2288.
[28] C. Jeronimo, R. Henrique, M.O. Hoque, E. Mambo, F.R. Ribeiro, G. Varzim, J. Oliveira, M.R. Teixeira, C. Lopes, D. Sidransky, A quantitative promoter methylation profile of prostate cancer, Clin. Cancer Res. 10 (2004) 8472–8478.
[29] M.J. Fackler, M. McVeigh, J. Mehrotra, M.A. Blum, J. Lange, A. Lapides, E. Garrett, P. Argani, S. Sukumar, Quantitative multiplex methylation-specific PCR assay for the detection of promoter hypermethylation in multiple genes in breast cancer, Cancer Res. 64 (2004) 4442–4452.
[30] M. Ehrich, M.R. Nelson, P. Stanssens, M. Zabeau, T. Liloglou, G. Xinarianos, C.R. Cantor, J.K. Field, D. van den Boom, Quantitative high-throughput analysis of DNA methylation patterns by base-specific cleavage and mass spectrometry, Proc. Natl. Acad. Sci. USA 102 (2005) 15785–15790.
[31] M. Frommer, L.E. McDonald, D.S. Millar, C.M. Collis, F. Watt, G.W. Grigg, P.L. Molloy, C.L.A. Paul, Genomic sequencing protocol that yields a positive display of 5-methylcytosine residues in individual DNA strands, Proc. Natl. Acad. Sci. USA 89 (1992) 1827–1831.
[32] R. Feil, J. Charlton, A.P. Bird, J. Walter, W. Reik, Methylation Analysis on Individual Chromosomes - Improved Protocol for Bisulfite Genomic Sequencing, Nucleic Acids Res. 22 (1994) 695–696.
[33] W.G. Han, B.T. Pentecost, S.D. Spivack, Functional evaluation of novel single nucleotide polymorphisms and haplotypes in the promoter regions of CYP1B1 and CYP1A1 genes, Mol. Carcinogen. 37 (2003) 158–169.
[34] V.K. Rakyan, T. Hildemann, K.L. Novik, J. Lewin, J. Tost, A.V. Cox, T.D. Andrews, K.L. Howe, T. Otto, A. Olek, J. Fischer, I.G. Gut, K. Berlin, S. Beck, DNA methylation profiling of the human major histocompatibility complex: A pilot study for the human epigenome project, PLoS Biol. 2 (2004) e405.

[35] J. Lewin, A.O. Schmitt, P. Adorjan, T. Hildmann, C. Piepenbrock, Quantitative DNA methylation analysis based on four-dye trace data from direct sequencing of PCR amplificates, Bioinformatics 20 (2004) 3005–3012.

[36] G.J. Hurteau, S.D. Spivack, mRNA-specific reverse transcription-polymerase chain reaction from human tissue extracts, Anal. Biochem. 307 (2002) 304–315.

[37] S. Mulero-Navarro, J.M. Carvajal-Gonzalez, M. Herranz, E. Ballestar, M.F. Fraga, S. Ropero, M. Esteller, P.M. Fernandez-Salguero, The dioxin receptor is silenced by promoter hypermethylation in human acute lymphoblastic leukemia through inhibition of Sp1 binding, Carcinogenesis 12 (2006) [Epub ahead of print].

[38] U. Deligezer, N. Erten, E.E. Akisik, N. Dalay, Methylation of the INK4A/ARF locus in blood mononuclear cells, Ann. Hematol. 85 (2006) 102–107.

[39] J.T. Attwood, R.L. Yung, B.C. Richardson, DNA methylation and the regulation of gene transcription, Cell. Mol. Life Sci. 59 (2002) 241–257.

[40] M. Ehrlich, Expression of various genes is controlled by DNA methylation during mammalian development, J. Cell. Biochem. 88 (2003) 899–910.

[41] S.J. Clark, J. Harrison, C.L. Paul, M. Frommer, High-sensitivity mapping of methylated cytosines, Nucleic Acids Res. 22 (1994) 2990–2997.

[42] L. Liu, R.C. Wylie, N.J. Hansen, L.G. Andrews, T.O. Tollefsbol, Profiling DNA methylation by bisulfite genomic sequencing: problems and solutions, Methods Mol. Biol. 287 (2004) 169–179.

[43] A. Meissner, A. Gnirke, G.W. Bell, B. Ramsahoye, E.S. Lander, R. Jaenisch, Reduced representation bisulfite sequencing for comparative high-resolution DNA methylation analysis, Nucleic Acids Res. 33 (2005) 5868–5877.

[44] S.D. Spivack, G.J. Hurteau, A.A. Reilly, K.M. Aldous, X.X. Ding, L.S. Kaminsky, CYP1B1 expression in human lung, Drug Metab. Disposition 29 (2001) 916–922.

[45] D.S. Millar, C.L. Paul, P.L. Molloy, S.J. Clark, A distinct sequence (ATAAA)(n) separates methylated and unmethylated domains at the 5′-end of the GSTP1 CpG island, J. Biol. Chem. 275 (2000) 24893–24899.

[46] S. Zochbauer-Muller, K.M. Fong, A.K. Virmani, J. Geradts, A.F. Gazdar, J.D. Minna, Aberrant promoter methylation of multiple genes in non-small cell lung cancers, Cancer Res. 61 (2001) 249–255.

[47] S. Toyooka, K.O. Toyooka, K. Miyajima, J.L. Reddy, M. Toyota, U.G. Sathyanarayana, A. Padar, M.S. Tockman, S. Lam, N. Shivapurkar, A.F. Gazdar, Epigenetic down-regulation of death-associated protein kinase in lung cancers, Clin. Cancer Res. 9 (2003) 3034–3041.